An Analytical Solution for Wellbore Heat Transmission in Layered Formations

Yu-Shu Wu,* SPE, and Karsten Pruess, SPE, Lawrence Berkeley Laboratory

Summary. This paper presents a new analytical solution for wellbore heat transmission. Previous treatments of the wellbore heat-transfer problem are improved in several aspects: (1) nonhomogeneous formations are approximated as layered formations with different physical properties; (2) closed-form analytical solutions are obtained in both real and Laplace space; and (3) a more accurate formula is provided for the transient heat-conduction function, $f(t_D)$.

Introduction

Heat is transferred to or from the wellbore when there is a difference in temperature between the surrounding formation and the injected (or produced) fluid. To evaluate the feasibility of a thermal recovery project, it is necessary to estimate the heat losses or gains of the flowing fluid in wellbores, the changes in temperature with time and depth, and the heat-transfer conditions between wellbore and formation. A quantitative description of heat exchange between a wellbore and surrounding formations often is also required when one attempts to estimate formation temperatures from wellbore measurements.

Studies of wellbore heat transmission during hot or cold fluid injection have appeared in the literature since the 1950's. The techniques available for dealing with wellbore heat transmission include analytical and numerical methods. Lessem et al.[1] and Squier et al.[2] derived and solved similar systems of differential equations describing the temperature behavior of gas and hot-water injection wells. They neglected wellbore thermal resistance and made the following assumptions.

1. No conductive heat transfer occurs in the vertical direction of either the flowing fluid or the formation.
2. The mass flow rate of gas or water is constant throughout the injection or production system.
3. The volumetric heat capacities of fluids and formation are constant.
4. The formation is homogeneous and isotropic with constant thermal conductivity.
5. The fluid temperature is the same as the formation temperature on the wellbore surface.

Subsequent work introduced another assumption, that vertical heat transfer in the wellbore was considered steady state.

The classic study by Ramey[3] on wellbore heat transmission improved Moss and White's[4] approach to incorporate an overall heat-transfer coefficient. Ramey presented an approximate solution for the temperatures of fluids, tubing, and casing as a function of time and depth in a well used for hot-fluid injection. Satter[5] suggested a similar method for analyzing wellbore heat loss when condensing steam flow is considered and provided a sample procedure for a given set of reservoir properties. Ramey[3] and Willhite[6] gave an expression for the overall heat-transfer coefficient for any well completion and the early-time values of the transient heat-conduction function. Durrant and Thambynayagam's[7] more recent work provided an iterative procedure for the wellbore heat-transmission problem during flow of steam/water mixtures that includes vertical heat conduction.

The numerical models by Farouq Ali[8] and Wooley[9] were more comprehensive than the analytical models. They include both horizontal and vertical heat conduction in the formation and can deal with different well operation conditions. The numerical methods, however, are often too complicated for field applications or for reservoir simulation studies because many of the required wellbore and formation heat-transfer properties are rarely known precisely.

*Now at Hydrogeologic Inc.

The mathematical model for wellbore heat transmission presented in this paper adopts assumptions similar to those of Lessem et al.[1] The main differences are that we introduce an overall heat-transfer coefficient to consider the wellbore heat resistance and that we treat the surrounding earth as consisting of an arbitrary number of layers with different thermal and physical properties and arbitrary initial temperature distributions (Fig. 1). An analytical solution has been obtained in both real and Laplace space for prediction of wellbore heat transmission. The numerical results calculated from the analytical solutions are compared with Ramey's long-time approximation. Illustrative applications are given for predicting wellbore heat transmission for engineering designs or reservoir simulation studies in petroleum and geothermal reservoir development.

Mathematical Model

The transient heat-transmission problem under consideration is illustrated in Fig. 1. The injection (or production) well is cased to the top of the injection (or production) interval. Heat is transferred along the wellbore solely by convection and then by conduction into the formation. The formation consists of n layers with different thermal and physical properties. The system is composed of three parts, as Fig. 1 shows: (1) fluid-flow conduit inside the tubing; (2) tubing/casing annulus, casing wall, and cement; and (3) infinite formation surrounding the casing. The major assumptions and approximations are as follows.

1. Fluid flow in the tubing is 1D, vertical, and steady with constant mass flow rate.
2. The well fluid temperature is lumped radially.
3. The vertical heat conduction is neglected compared with heat convection by the flowing fluid.
4. Radial heat flow between the wellbore and the formation is steady state.
5. In the surrounding earth, the initial geothermal gradient is a known function of depth.
6. The vertical heat conduction in the formation can be ignored compared with the horizontal heat flow.

All other assumptions are similar to those of previous work. Therefore, the heat-transfer equation in the tubing can be written as

$$\rho_t c_t(\partial T_{1j}/\partial t)+(2/r_t)q_j''+\rho_t c_t v_m(\partial T_{1j}/\partial z)=0,$$
$$j=1,2\ldots n\ (z_{j-1}<z<z_j) \quad\ldots\ldots\ldots\ldots\ldots\ldots\ldots\ldots\ldots(1)$$

for liquid flow and

$$\rho_t c_t(\partial T_{1j}/\partial t)+(2/r_t)q_j''+\rho_t c_t v_m[(\partial T_{1j}/\partial z)\pm(g/c_t)]=0,$$
$$j=1,2\ldots n\ (z_{j-1}<z<z_j) \quad\ldots\ldots\ldots\ldots\ldots\ldots\ldots\ldots\ldots(2)$$

for gas flow, where the plus sign on the potential-energy term is used for flow down the well and the negative sign is used for flow up the well.[3]

The heat conduction in Layer j of the formation is described by

$$(1/r)(\partial/\partial r)[rk_{hj}(\partial T_{2j}/\partial r)]=\rho_j c_j(\partial T_{2j}/\partial t),$$
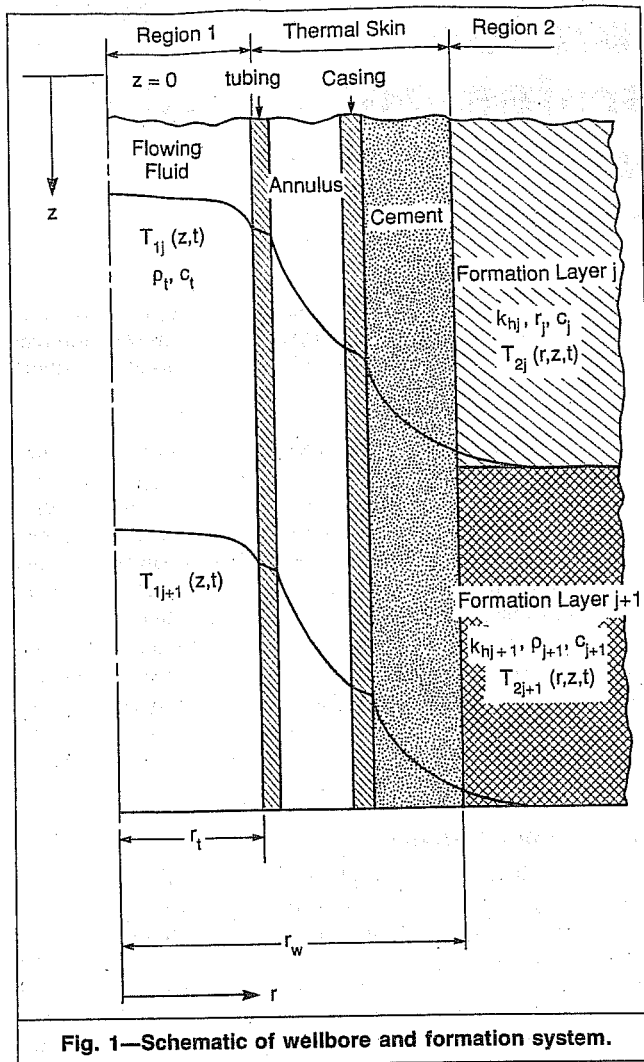$$j=1,2\ldots n\ (z_{j-1}<z<z_j). \quad\ldots\ldots\ldots\ldots\ldots\ldots\ldots\ldots(3)$$

Fig. 1—Schematic of wellbore and formation system.

The heat flux across the tubing surface is

$$q_j{''}=U_j(T_{1j}-T_{2j}|_{r=r_w}), \quad\ldots\ldots\ldots\ldots\ldots\ldots\ldots\ldots(4)$$

where U_j=overall heat-transfer coefficient defined by Ramey[3] and Willhite.[6]

The initial condition in the well are

$$T_{1j}(z,t=0)=T_{ij}(z)\text{(known functions)}, j=1,2\ldots n \ (z_{j-1}<z\le z_j),$$

$$\ldots\ldots\ldots\ldots\ldots\ldots\ldots\ldots\ldots\ldots\ldots\ldots\ldots(5)$$

and initial conditions in the formation are

$$T_{2j}(r;z,t=0)=T_{ij}(z), j=1,2\ldots n \ (z_{j-1}\le z\le z_j). \quad\ldots\ldots\ldots(6)$$

In Eqs. 5 and 6 it is required that

$$T_{i1}(0)=T_{air}; \quad\ldots\ldots\ldots\ldots\ldots\ldots\ldots\ldots\ldots\ldots\ldots\ldots(7)$$

i.e., the temperature on the ground is assumed constant.
The boundary conditions are

$$T_{11}(z=0,t)=T_{inj} \quad\ldots\ldots\ldots\ldots\ldots\ldots\ldots\ldots\ldots\ldots\ldots\ldots(8)$$

and $$\lim_{r\to\infty} T_{2j}(r,z,t)=T_{ij}(z), j=1,2\ldots n. \quad\ldots\ldots\ldots\ldots(9)$$

Analytical Solution

The dimensionless parameters for radial distance, time, and depth are

$$r_D=r/r_w, \quad\ldots\ldots\ldots\ldots\ldots\ldots\ldots\ldots\ldots\ldots\ldots\ldots\ldots\ldots\ldots(10)$$

$$t_D=tv_m/D, \quad\ldots\ldots\ldots\ldots\ldots\ldots\ldots\ldots\ldots\ldots\ldots\ldots\ldots\ldots(11)$$

and $$z_D=z/D. \quad\ldots\ldots\ldots\ldots\ldots\ldots\ldots\ldots\ldots\ldots\ldots\ldots\ldots\ldots(12)$$

The dimensionless temperature functions are

$$\theta_j(z_D,t_D)=[T_{1j}(z,t)-T_{ij}(z)]/(T_{inj}-T_{air}), j=1,2\ldots n, \quad\ldots(13)$$

in the wellbore and

$$\phi_j(r_D,z_D,t_D)=[T_{2j}(r,z,t)-T_{ij}(z)]/[(T_{inj}-T_{air})], j=1,2\ldots n,$$

$$\ldots\ldots\ldots\ldots\ldots\ldots\ldots\ldots\ldots\ldots\ldots\ldots\ldots\ldots(14)$$

in the formation.

The unsteady-state solution of this system in Laplace space becomes (Appendix A)

$$\bar\theta_j(z_D,s)=C_j(s)\exp\{-[s+\beta_j-D_j(s)]z_D\}$$
$$+Y_j(z_D,s), j=1,2\ldots n, \quad\ldots\ldots\ldots\ldots\ldots\ldots\ldots\ldots\ldots(15)$$

where $C_1(s)=(1/s)+[\delta_1(z_D)]/s[s+\beta_1-D_1(s)], \quad\ldots\ldots\ldots\ldots(16)$

$$C_j(s)=\left\{\bar\theta_{j-1}(z_{D_{j-1}},s)+\frac{\delta_j(z_D)}{s[s+\beta_j-D_j(s)]}\right\}$$

$$\times\exp\{[s+\beta_j-D_j(s)]z_{D_{j-1}}\}, j=2,3\ldots n, \quad\ldots\ldots\ldots\ldots(17)$$

and $\bar\phi_j(r_D,z_D,s)=[\omega_j\bar\theta_j(z_D,s)K_0(\sqrt{\sigma_j s}\,r_D)]/$

$$[\omega_j K_0(\sqrt{\sigma_j s})+\sqrt{\sigma_j s}\,K_1(\sqrt{\sigma_j s})], j=1,2\ldots n. \quad\ldots\ldots\ldots(18)$$

The functions $Y_j(z,s)$, $D_j(s)$, and $\delta_j(z_D)$ and the parameters β_j, ω_j, and σ_j are defined in Appendix A. The temperature function, $\bar\theta_j$, in Laplace space can be determined recursively from Layer j to $j+1$ ($j=1,2\ldots n-1$) because it is assumed that there is no vertical heat conduction in either the wellbore or the formation. Therefore, downstream wellbore fluid or formation temperatures have no effect on upstream temperatures.

Another important variable of interest for wellbore heat transmission is the heat flow rate transferred into (or from) the formation. For a linear initial temperature distribution in each layer of the formation,

$$T_{ij}(z)=T_{cj}+g_{g,j}z, \quad\ldots\ldots\ldots\ldots\ldots\ldots\ldots\ldots\ldots\ldots\ldots(19)$$

where the T_{cj} are constant. Continuity at the interfaces of layers requires that

$$T_{c1}=T_{air} \quad\ldots\ldots\ldots\ldots\ldots\ldots\ldots\ldots\ldots\ldots\ldots\ldots\ldots(20)$$

and $T_{cj}+g_{g,j}z_j=T_{cj+1}+g_{g,j+1}z_j, j=1,2\ldots n-1. \quad\ldots\ldots(21)$

Then $T_{ij}'(z)=g_{g,j} \quad\ldots\ldots\ldots\ldots\ldots\ldots\ldots\ldots\ldots\ldots\ldots\ldots(22)$

and $Y_j(z_D,s)=-[\delta_j/s(s+\beta_j-D_j(s)]. \quad\ldots\ldots\ldots\ldots\ldots\ldots(23)$

For the heat flux into (or from) the formation, in Laplace space,

$$\bar q_j{''}(z,s)=-U_j(T_{inj}-T_{air})[\bar\phi_j(1,z_D,s)-\bar\theta_j(z_D,s)], j=1,2\ldots n.$$

$$\ldots\ldots\ldots\ldots\ldots\ldots\ldots\ldots\ldots\ldots\ldots\ldots\ldots\ldots(24)$$

The cumulative heat flow rate is

$$\bar Q_c(s)=\frac{2\pi r_t D^2(T_{inj}-T_{air})}{v_m}\sum_{j=1}^{n}\frac{U_j}{s}\left[1-\frac{D_j(s)}{\beta_j}\right]$$

$$\times\left[\left\{\bar\theta_{j-1}(z_{Dj-1},s)+\frac{\delta_j}{s[s+\beta_j-D_j(s)]}\right\}\right.$$

$$\times\left(1-\exp\{-[s+\beta_j-D_j(s)](z_{Dj}-z_{Dj-1})\}\right)$$

$$\left.\div[s+\beta_j-D_j(s)]-\frac{\delta_j}{s[s+\beta_j-D_j(s)]}(z_{Dj}-z_{Dj-1})\right]. \quad\ldots\ldots(25)$$

The solutions in Laplace space can be evaluated by numerical inversion techniques.[10] Analytical solutions in real space are desirable for validating the numerical inversion results and for predicting the early-time transient behavior of the system because the numerical Laplace transform cannot be expected to give accurate results for early time. We have obtained solutions in real space for a linear initial temperature distribution in each formation layer in

TABLE 1—CALCULATION DATA	
g_g, °C/m [°F/ft]	0.03 [0.016]
T_{inj}, °C [°F]	100 [212]
Q, m³/d [ft³/D]	100 [3,531]
ρ_w, kg/m³ [lbm/ft³]	958 [59.8]
U, W/(m²·°C) [Btu/(ft²·°F)]	978 [172]
T_{air}, °C [°F]	20 [68]
D, m [ft]	1,000 [3,281]
r_w, m [ft]	0.08 [0.26]*
c_w, J/(kg·°C) [Btu/(lbm·°F)]	4196 [1.00]
Sandstone	
ρ, kg/m³ [lbm/ft³]	2200 [137.3]
c, J/(kg·°C) [Btu/(lbm·°F)]	740 [0.167]
K, W/(m·°C) [Btu/(ft-hr·°F)]	2.8 [1.62]
Clay	
ρ, kg/m³ [lbm/ft³]	1500 [93.6]
c, J/(kg·°C) [Btu/(lbm·°F)]	800 [0.191]
K, W/(m·°C) [Btu/(ft-hr·°F)]	1.4 [0.81]

*16.08-cm [6.33-in.] ID.

Fig. 2—Comparison of numerical inversion of Laplace transformation with exact solution and Ramey's solution.

Appendix B. For Layer 1 ($0 \leq z_D \leq z_{D1}$) or for a homogeneous formation we have

$$\theta_1(z_D,t_D) = \begin{cases} I_1 & (t_D \leq z_D) \\ I_1 + I_2 + I_3 & (t_D > z_D) \end{cases}, \quad \dots \dots \dots \dots (26)$$

where

$$I_1 = \frac{4\delta_1}{\pi^2} \int_0^\infty \frac{D_1^*(u)}{u} \frac{\left[\exp\left(-\frac{u^2}{\sigma_1}t_D\right) - 1\right]}{\left\{\left[D_1^*(u)\left(\beta_1 - \frac{u^2}{\sigma_1}\right) - R_1(u)\right]^2 + \frac{4}{\pi^2}\right\}} du,$$

$$\dots \dots \dots \dots \dots \dots (27)$$

$$I_2 = \frac{2e^{-\beta_1 z_D}}{\pi} \int_0^\infty \frac{\left\{1 - \exp\left[-\frac{u^2}{\sigma_1}(t_D - z_D)\right]\right\}}{u}$$

$$\times \exp[z_D R_1(u)/D_1^*(u)]\sin\left[\frac{2z_D}{\pi D_1^*(u)}\right]du, \quad \dots \dots \dots (28)$$

and

$$I_3 = \frac{2\delta_1 e^{-\beta_1 z_D}}{\pi} \int_0^\infty \frac{D_1^*(u)\left\{1 - \exp\left[-\frac{u^2}{\sigma_1}(t_D - z_D)\right]\right\}}{u\left\{\left[D_1^*(u)\left(\beta_1 - \frac{u^2}{\sigma_1}\right) - R(u)\right]^2 + \frac{4}{\pi^2}\right\}}$$

$$\times \exp[z_D R_1(u)/D_1^*(u)]\left\{\frac{2}{\pi}\cos\left[\frac{2z_D}{\pi D_1^*(u)}\right] + \sin\left[\frac{2z_D}{\pi D_1^*(u)}\right]\right\}$$

$$\times \left[D_1^*(u)\left(\beta_1 - \frac{u^2}{\sigma_1}\right) - R_1(u)\right]\right\}du. \quad \dots \dots \dots \dots (29)$$

For Layer $j = 2,3 \dots n$, the dimensionless wellbore temperatures are

$$\theta_j(z_D,t_D) = A_j(t_D) + \int_0^{t_D}[\theta_{j-1}(z_{Dj-1},\tau) - A_j(\tau)]B_j(z_D,t_D-\tau)d\tau,$$

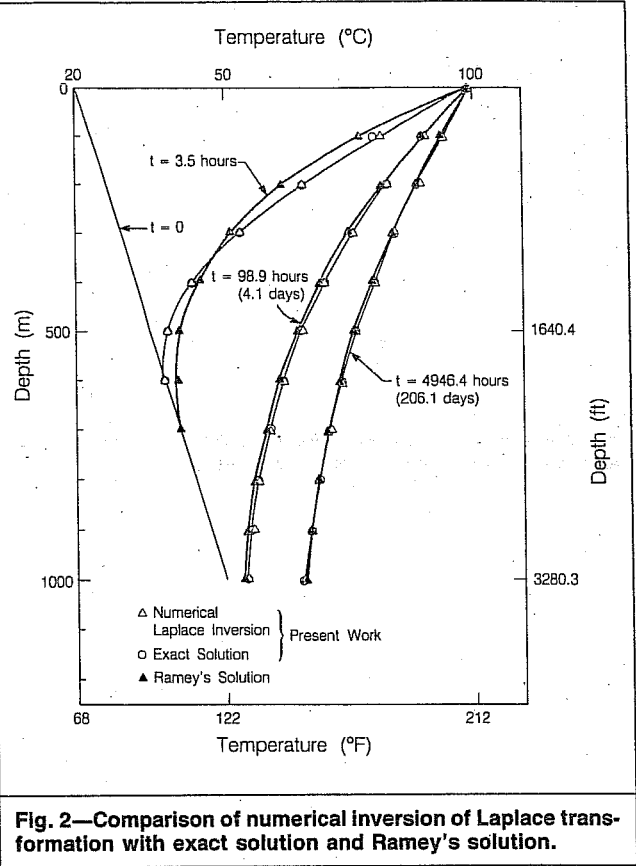$$\dots \dots \dots \dots \dots \dots \dots \dots (30)$$

where $A_j(t_D) = \frac{4\delta_j}{\pi^2} \int_0^\infty$

$$\times \frac{D_j^*(u)}{u} \frac{\left[\exp\left(-\frac{u}{\sigma_1}t_D\right) - 1\right]}{\left\{\left[D_j^*(u)\left(\beta_j - \frac{u^2}{\sigma_j}\right) - R_j(u)\right]^2 + \frac{4}{\pi^2}\right\}} du, \quad \dots (31)$$
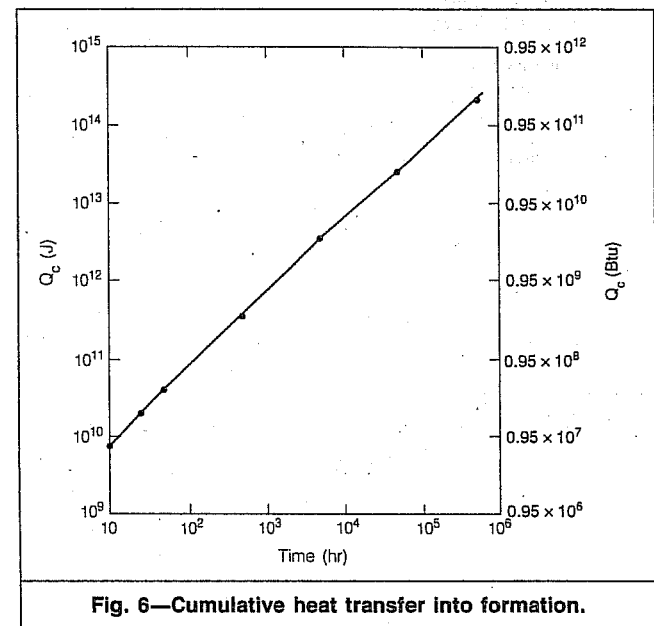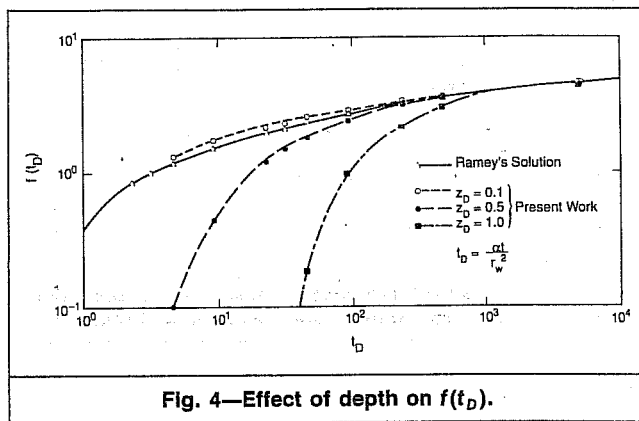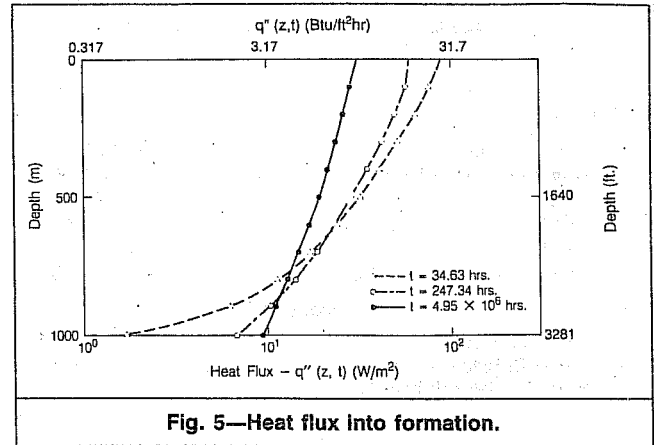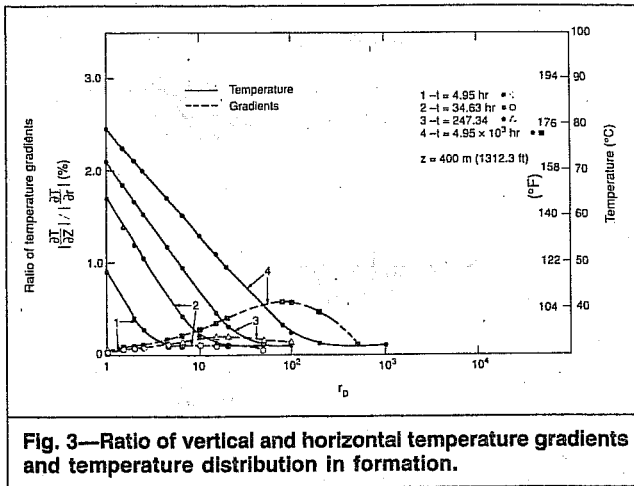
and $B_j(z_D,t_D) =$

$$\begin{cases} 0 & (t_D \leq z_D - z_{Dj-1}) \\ \\ \frac{2}{\pi\sigma_j}\exp[-\beta_j(z_D-z_{Dj-1})]\int_0^\infty u \sin\left[\frac{2(z_D-z_{Dj-1})}{\pi D_j^*(u)}\right] \\ \times \exp\left[(z_D - z_{Dj-1})R_j(u)/D_j^*(u) - \frac{u^2}{\sigma_j}(t_D - z_D + z_{Dj-1})\right]du, \\ t_D > z_D - z_{Dj-1}. \end{cases}$$

$$\dots \dots \dots \dots \dots \dots \dots \dots (32)$$

$R_j(u)$ and $D_j^*(u)$ in Eqs. 27 through 32 are defined in Appendix B. The dimensionless temperature function in Layer j is given by

$$\phi_j(r_D,z_D,t_D) = \int_0^{t_D} \theta_j(z_D,\tau)g_j(r_D,t_D-\tau)d\tau, \quad \dots \dots \dots (33)$$

where $g_j(r_D,t_D) = \frac{2}{\pi\sigma_j\beta_j}\int_0^\infty \frac{u}{D_j^*(u)}\exp\left(-\frac{u^2}{\sigma_j}t_D\right)$

$$\times \left\{Y_0(ur_D)[\omega_j J_0(u) + uJ_1(u)] - J_0(ur_D)[uY_1(u) + \omega_j Y_0(u)]\right\}du.$$

$$\dots \dots \dots \dots \dots \dots \dots \dots (34)$$

Fig. 3—Ratio of vertical and horizontal temperature gradients and temperature distribution in formation.

Fig. 5—Heat flux into formation.

Fig. 4—Effect of depth on $f(t_D)$.

Fig. 6—Cumulative heat transfer into formation.

Discussion

A series of tests were conducted to validate the analytical solutions. The numerical inversion results of the Laplace-transformed solution of Eq. 15 were compared with the numerical integration of the exact solution of Eq. 26 and with Ramey's long-time solution. The integrals in Eq. 26 were calculated with the numerical integral-evaluation routine from the NAG Fortran Library[11] on a CRAY computer. Convergence of the numerical integration was very rapid and smooth.

The example problem is a hot-water injection at a constant rate. Table 1 gives the fluid and formation data for the calculation. As Fig. 2 shows, the numerical Laplace inversion results are in excellent agreement with the exact solution, and at long times, both the solution and Ramey's solution converge to the same curve.

The results from the numerical Laplace inversion by the Stehfest algorithm generally need to be checked against some other solution, particularly for early times. We have found that the numerical inversion gives very poor results for the early times when $t_D \leq z_D$. This probably occurs because of the rapidly changing condition at the sandface until the entire wellbore is full of injected water when $t_D > 1$. At later times, the numerical inversion will give very accurate results. Therefore, the exact solution in real space, instead of that in Laplace space, should be used for applications in which early-time transient behavior is important, such as in temperature well logging analysis.[12]

As in most studies on wellbore heat transfer, the vertical heat conduction is ignored here because it is negligible compared with horizontal flow. We examine this approximation by comparing the horizontal and vertical temperature gradients in the formation derived from the solutions obtained above. As Fig. 3 shows, the ratio of vertical and horizontal temperature gradients is always smaller than 1%, and reaches its maximum around the temperature penetration fronts. A larger vertical heat flow may occur on the interface of formation layers with different properties where the temperatures obtained by neglecting vertical flow are vertically discontinuous.

We found that the difference in temperatures is very small on the interface of the sandstone and clay whose properties are given in Table 1. These results should be conservative because vertical temperature differences are overestimated if vertical flow is neglected. Therefore, the assumption that the vertical heat flow in the formation is negligible is probably acceptable for most engineering calculations.

A steady-state approximation for vertical heat transfer in the wellbore has been made in almost all previous wellbore heat-transfer models. This approximation is not needed here. It has been shown that the steady-state treatment overestimates the temperature increase in the wellbore at early times but that the differences disappear at long times.

The transient heat-conduction function, $f(t_D)$, discussed in detail by Ramey[3] and Willhite,[6] is widely used for wellbore heat-transfer calculations. However, only an approximate analytical expression for $f(t_D)$, which is based on the long-time line-source solution from Ramey, is available in the literature. We obtain an accurate formula for $f(t_D)$ as a special case of applications of the analytical solution to a uniform and homogeneous formation (subscripts omitted):

$$f(t_D) = \frac{2\pi K[T_2|_{r=r_w} - T_i(z)]}{dq''/dz} = \frac{\phi(1, z_D, t_D)}{\omega[\theta(z_D, t_D) - \phi(1, z_D, t_D)]}.$$

$$\dots\dots\dots\dots\dots\dots\dots\dots\dots\dots\dots\dots\dots (35)$$

It is interesting to note that in a more rigorous formulation, $f(t_D)$ is a function not only of dimensionless time, t_D, but also of dimensionless depth, z_D. This can be seen explicitly from Fig. 4, in

which $f(t_D)$ from Eq. 35 is plotted for different z_D. Only after $t_D \geq 500$ (2,500 hours for this case) does $f(t_D)$ become independent of z_D. This means that the use of an $f(t_D)$ independent of z_D will not give accurate results during the early transient time for wellbore heat-transfer problems.

Heat loss (or gain) from wells is important for evaluating a thermal recovery project. **Figs. 5 and 6** show the behavior of heat flux and cumulative heat transfer into the surrounding formation for hot-water injection into a well in a homogeneous sandstone formation. Table 1 gives the calculation parameters. Fig. 6 clearly shows that the heat losses from the well and the temperatures never reach a steady state because the formation is modeled as an infinite radial system.

In an actual reservoir, formations are neither uniform nor homogeneous, and layered formations may be a realistic approximation. To take into account effects of formation heterogeneity on wellbore heat transfer, the temperature distribution along the wellbore was calculated for hot-water injection into a formation consisting of two layers. The upper 500 m [1,640 ft] is sandstone, and the lower 500 m [1,640 ft] is clay. Table 1 gives the problem parameters. As **Fig. 7** shows, if only sandstone properties are used, well temperatures are underestimated because thermal diffusivity in sandstone is larger than that in clay. Fig. 7 suggests that the assumption of constant formation properties introduces errors for nonhomogeneous reservoirs.

Conclusions

An analytical solution for determining wellbore heat transfer has been developed that is applicable to field predictions and reservoir simulation studies of wellbore heat transmission in uniform and layered formations. Illustrative examples were given for temperature distributions along the wellbore and in the formation, and for heat-transfer rates and cumulative heat loss (or gain) between wellbore and formation. Analysis of the calculated results of the analytical solution leads to the following conclusions.

1. Vertical heat conduction in the formation may be ignored for engineering applications.

2. The use of a depth-independent heat-conduction function, $f(t_D)$, will introduce large errors at early times in calculations of wellbore temperature.

3. Effects of formation heterogeneity should be included for more accurate predictions of wellbore heat transmission in nonhomogeneous formations.

Nomenclature

$$
\begin{aligned}
A_j(t_D) &= \text{defined in Eq. 31} \\
\bar{A}_j(s) &= \text{defined in Eq. B-2} \\
B_j(z_D,t_D) &= \text{defined in Eq. 32} \\
\bar{B}_j(z_D,s) &= \text{defined in Eq. B-3} \\
c_j &= \text{formation specific heat of Layer } j, \text{ J/kg} \cdot {}^\circ\text{C} \\
&\quad [\text{Btu/(lbm-}{}^\circ\text{F)}] \\
c_t &= \text{fluid specific heat in tubing, J/(kg} \cdot {}^\circ\text{C)} \\
&\quad [\text{Btu/(lbm-}{}^\circ\text{F)}] \\
C_j &= \text{constant in Eqs. A-23 and A-24} \\
D &= \text{depth to top of permeable interval, m [ft]} \\
D_j(s) &= \text{defined in Eq. A-25} \\
D_j^*(u) &= \text{defined in Eq. B-15} \\
f(t_D) &= \text{transient heat-conduction function defined in} \\
&\quad \text{Eq. 35} \\
f_j(t_D) &= \text{defined in Eq. B-7} \\
\bar{f}_j(s) &= \text{defined in Eq. B-2} \\
g &= \text{acceleration of gravity, m/s}^2 \text{ [ft/sec}^2] \\
g_{g,j} &= \text{geothermal gradient of Layer } j, {}^\circ\text{C/m [}{}^\circ\text{F/ft]} \\
g_j(r_D,t_D) &= \text{defined in Eq. B-12} \\
\bar{g}_j(r_D,s) &= \text{defined in Eq. B-6} \\
i &= \text{injection rate, m}^3/\text{s [B/D]} \\
I_j &= \text{defined in Eqs. 27 through 29 } (j=1,2,3) \\
J_0 &= \text{zero-order Bessel function of first kind} \\
J_1 &= \text{first-order Bessel function of first kind} \\
k_h &= \text{thermal conductivity of formation, W/(m} \cdot {}^\circ\text{C)} \\
&\quad [\text{Btu/(hr-ft}^2\text{-}{}^\circ\text{F/in.)}]
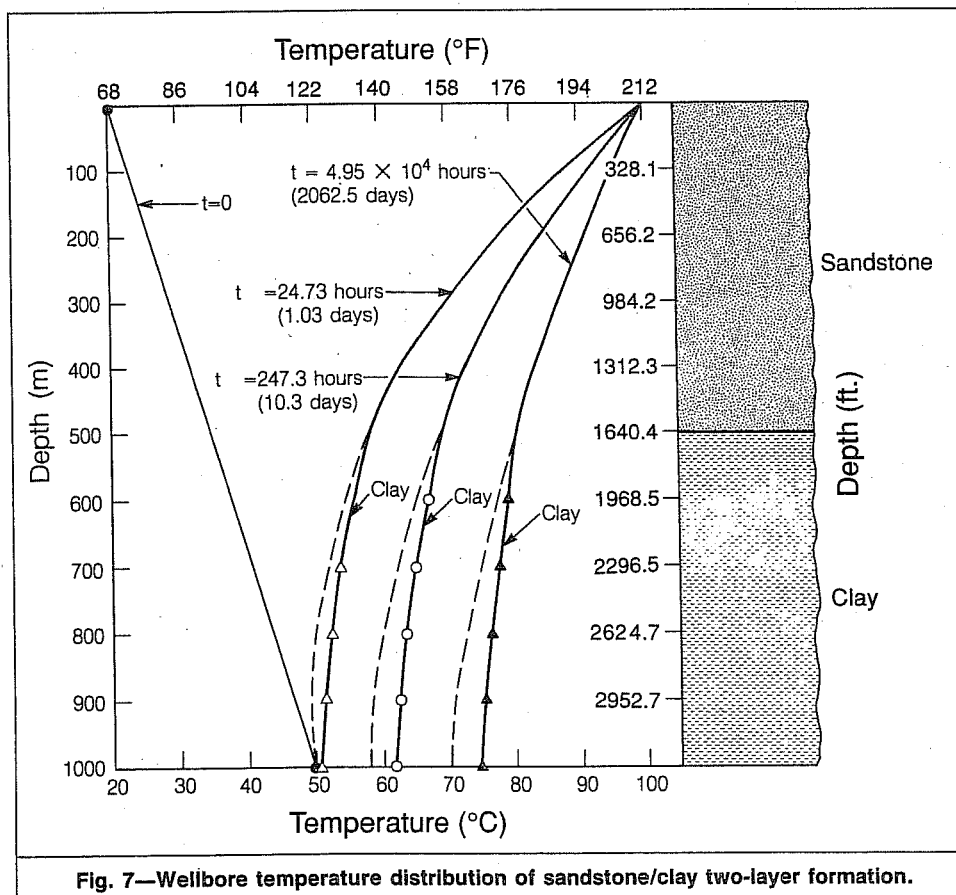\end{aligned}
$$

Fig. 7—Wellbore temperature distribution of sandstone/clay two-layer formation.

k_{hj} = thermal conductivity of Layer j formation, W/(m·°C) [Btu/(hr-ft²-°F/in.)]

K_0 = zero-order modified Bessel function of second kind

K_1 = first-order modified Bessel function of second kind

n = total formation layer number with different physical properties

q'' = heat flux between tubing and sandface, W/m² [Btu/ft²·hr]

$\bar{q}_j''(z,s)$ = defined in Eq. 24

Q_c = cumulative heat exchange between well and formation, J [Btu]

$\bar{Q}_c(s)$ = defined in Eq. 25

r = radius, m [ft]

r_D = dimensionless radius defined in Eq. 10

r_t = inside radius of tubing, m [ft]

r_w = outside radius of cement zone, m [ft]

$R_j(u)$ = defined in Eq. B-14

s = Laplace transform variable

t = time, seconds

t_D = dimensionless time defined in Eq. 11

T = temperature, °C [°F]

T_{air} = surface temperature, °C [°F]

T_{cj} = constant temperature in $T_{ij}(z)$, °C [°F]

$T_{ij}(z)$ = initial temperature as a function of depth, °C [°F]

T_{inj} = surface injection fluid temperature, °C [°F]

$T_{1j}(z,t)$ = temperature along tubing, °C [°F]

$T_{2j}(r,z,t)$ = temperature in formation, °C [°F]

U_j = overall heat-transfer coefficient, W/(m²·°C) [Btu/(hr-ft²-°F)]

v_m = mean flow speed inside tubing, m/s [ft/sec]

$Y_j(z_D,s)$ = particular solution in Eq. 21

Y_0 = zero-order Bessel function of second kind

Y_1 = first-order Bessel function of second kind

z = vertical coordinate, m [ft]

z_D = dimensionless vertical coordinate defined in Eq. 12

z_{Dj} = z_j/H, dimensionless depth of Layer j, (j=1,2...n)

z_j = depth of bottom of Layer j, (j=1,2...n, z_0=0)

α = thermal diffusivity of formation (α=$K/\rho c$), m²/s [ft²/sec]

β_j = dimensionless constant (Eq. A-3)

$\delta_j(z_D)$ = defined in Eq. A-4

$\theta_j(z_D,t_D)$ = dimensionless temperature functions of wellbore

$\xi_j(z_D)$ = dimensionless function (Eq. A-5)

ρ = density, kg/m³ [lbm/ft³]

ρ_t = fluid density in tubing, kg/m³ [lbm/ft³]

σ_j = dimensionless constant (Eq. A-6)

$\phi_j(r_D,z_D,t_D)$ = dimensionless temperature function of formation

ω_j = defined in Eq. A-13

Subscripts

D = dimensionless

j = formation layer index (j=1,2...n)

1 = in tubing

2 = in formation

Superscripts

$^-$ = Laplace space

Acknowledgment

We are indebted to Paul Witherspoon and Jahan Noorishad for careful review of the manuscript. This work was supported by the Assistant Secretary for Conservation & Renewable Energy, Office of

References

1. Lessem, L.B. *et al.*: "A Method of Calculating the Distribution of Temperature in Flowing in Gas Wells," *Trans.*, AIME (1957) **210**, 169–72.
2. Squier, D.P., Smith, D.D., and Dougherty, E.L.: "Calculated Temperature Behavior of Hot-Water Injection Wells," *JPT* (April 1962) 436–40; *Trans.*, AIME, **225**.
3. Ramey, H.J. Jr.: "Wellbore Heat Transmission," *JPT* (April 1962) 427–35; *Trans.*, AIME, **225**.
4. Moss, J.T. and White, P.D.: "How To Calculate Temperature Profiles in a Water-Injection Well," *Oil & Gas J.* (March 9, 1959) **57**, No. 11, 174–78.
5. Satter, A.: "Heat Losses During Flow of Steam Down a Wellbore," *JPT* (July 1965) 845–51; *Trans.*, AIME, **234**.
6. Willhite, G.P.: "Over-All Heat Transfer Coefficients in Steam and Hot Water Injection Wells," *JPT* (May 1967) 607–15.
7. Durrant, A.J. and Thambynayagam, R.K.M.: "Wellbore Heat Transmission and Pressure Drop for Steam/Water Injection and Geothermal Production: A Simple Solution Technique,'" *SPERE* (March 1986) 148–57.
8. Farouq Ali, S.M.: "A Comprehensive Wellbore Steam/Water Flow Model for Steam Injection and Geothermal Applications," *SPEJ* (Oct. 1981) 527–34.
9. Wooley, G.R.: "Computing Downhole Temperatures in Circulation, Injection, and Production Wells," *JPT* (Sept. 1980) 1509–22.
10. Stehfest, H.: "Numerical Inversion of Laplace Transforms," *Communications, ACM* (Jan. 1970) **13**, No. 1, 47–49.
11. *NAG FORTRAN Library Manual, Mark 11*, Numerical Algorithms Group (1984) **1**, Chap. D01.
12. Barelli, A. and Palama, A.: "A New Method for Evaluating Formation Equilibrium Temperature in Holes During Drilling," *Geothermics* (1981) **10**, No. 2, 95–102.
13. Carslaw, H.S. and Jaeger, J.C.: *Conduction of Heat in Solids*, second edition, Oxford U. Press, London (1959) 297–304.
14. Hildebrand, F.B.: *Advanced Calculus for Applications*, second edition, Prentice-Hall Inc., Englewood Cliffs, NJ (1976) 625–28.

Appendix A—Analytical Solution in Laplace Space

In terms of the dimensionless variables defined in Eqs. 10 through 14, the problem becomes

$$\frac{\partial \theta_j}{\partial t_D} + \frac{\partial \theta_j}{\partial z_D} + \beta_j(\theta_j - \phi_j|_{r_D=1}) + \delta_j(z_D) = 0 \quad \ldots\ldots\ldots\ldots \text{(A-1)}$$

and $$\frac{\partial^2 \phi_j}{\partial r_D^2} + \frac{1}{r_D}\frac{\partial \phi_j}{\partial r_D} = \sigma_j \frac{\partial \phi_j}{\partial t_D}, \quad \ldots\ldots\ldots\ldots\ldots\ldots \text{(A-2)}$$

where j=1,2...n and

$$\beta_j = 2U_j D/\rho_t c_t r_t v_m, \quad \ldots\ldots\ldots\ldots\ldots\ldots\ldots\ldots \text{(A-3)}$$

$$\delta_j(z_D) = \begin{cases} \xi_j(z_D) & \text{for liquid flow} \\ \xi_j(z_D) \pm D_g/(T_{inj} - T_{air})c_t & \text{for gas flow} \end{cases}, $$
$$\ldots\ldots\ldots\ldots\ldots\ldots\ldots\ldots\ldots\ldots\ldots\ldots\ldots \text{(A-4)}$$

$$\xi_j(z_D) = DT_{ij}'(z)/(T_{inj} - T_{air}), \quad \ldots\ldots\ldots\ldots\ldots\ldots \text{(A-5)}$$

and $$\sigma_j = \rho_t c_j v_m r_w^2/Dk_{hj}, \quad \ldots\ldots\ldots\ldots\ldots\ldots\ldots\ldots \text{(A-6)}$$

with initial conditions

$$\theta_j(z_D,t_D=0) = 0 \quad \ldots\ldots\ldots\ldots\ldots\ldots\ldots\ldots\ldots \text{(A-7)}$$

and $$\phi_j(r_D,z_D,t_D=0) = 0 \quad \ldots\ldots\ldots\ldots\ldots\ldots\ldots\ldots \text{(A-8)}$$

and boundary conditions

$$\theta_1(z_D=0,t_D) = 1, \quad \ldots\ldots\ldots\ldots\ldots\ldots\ldots\ldots\ldots \text{(A-9)}$$

$$\theta_j(z_{Dj-1},t_D) = \theta_{j-1}(z_{Dj-1},t_D), j=2,3\ldots n, \quad \ldots\ldots\ldots \text{(A-10)}$$

$$\partial\phi_j/\partial r_D|_{r_D=1} = \omega_j(\phi_j|_{r_D=1} - \theta_j), \quad \ldots\ldots\ldots\ldots\ldots \text{(A-11)}$$

and $$\lim_{r_D \to \infty} \phi_j(r_D,z_D,t_D) = 0. \quad \ldots\ldots\ldots\ldots\ldots\ldots \text{(A-12)}$$

In Eq. A-11,

$$\omega_j = U_j r_t / k_j. \quad \ldots\ldots\ldots\ldots\ldots\ldots (A\text{-}13)$$

The Laplace transforms of $\theta_j(z_D,t_D)$ and $\phi_j(r_D,z_D,t_D)$ are defined as follows[13]:

$$\bar{\theta}_j(z_D,s) \int_0^\infty \theta(z_D,t_D)e^{-t_D s}dt_D, \; j=1,2\ldots n \quad \ldots\ldots\ldots (A\text{-}14)$$

and $\displaystyle \bar{\phi}_j(r_D,z_D,s) = \int_0^\infty \phi_j(r_D,z_D,t_D)e^{-t_D s}dt_D, \; j=1,2\ldots n.$

$$\ldots\ldots\ldots\ldots\ldots\ldots\ldots\ldots\ldots (A\text{-}15)$$

Application of the Laplace transformation to partial-differential Eqs. A-1 and A-2 and boundary conditions in Eqs. A-9 through A-12 with incorporation of the initial conditions in Eqs. A-7 and A-8 yields

$$d\bar{\theta}_j/dz_D + (s+\beta_j)\bar{\theta}_j - \beta_j\bar{\phi}_j|_{r_D=1} + [\delta_j(z_D)/s] = 0, \quad \ldots (A\text{-}16)$$

$$(d^2\bar{\phi}_j/dr_D^2) + (1/r_D)(d\bar{\phi}_j/dr_D) - \sigma_j s\bar{\phi}_j = 0, \quad \ldots\ldots\ldots (A\text{-}17)$$

$$d\bar{\phi}_j/dr_D|_{r_D=1} = \omega_j(\bar{\phi}_j|_{r_D=1} - \bar{\theta}_j), \quad \ldots\ldots\ldots\ldots (A\text{-}18)$$

$$\bar{\theta}_1(z_D=0,s) = 1/s, \quad \ldots\ldots\ldots\ldots\ldots\ldots\ldots\ldots (A\text{-}19)$$

and $\bar{\theta}_j(z_{Dj-1},s) = \bar{\theta}_{j-1}(z_{Dj-1},s), \quad \ldots\ldots\ldots\ldots (A\text{-}20)$

where $j=1,2\ldots n$. The solutions of Eqs. A-16 and A-17 in Laplace space, satisfying the boundary condition of Eqs. A-18 through A-20, are

$$\bar{\theta}_j(z_D,s) = C_j(s)\exp\{-[s+\beta_j-D_j(s)]z_D\} + Y_j(z_D,s) \quad \ldots (A\text{-}21)$$

and $\bar{\phi}_j(r_D,z_D,s) =$

$$\omega_j\bar{\theta}_j(z_D,s)K_0(\sqrt{\sigma_j s}\,r_D)/[\omega_j K_0(\sqrt{\sigma_j s}) + \sqrt{\sigma_j s}\,K_1(\sqrt{\sigma_j s})],$$

$$\ldots\ldots\ldots\ldots\ldots\ldots\ldots\ldots\ldots (A\text{-}22)$$

where the $Y_j(z_D,s)$ are the particular solutions of Eq. A-16 that depend on the initial temperature profile.

$$C_1 = (1/s) - Y_1(z_D=0,s), \quad \ldots\ldots\ldots\ldots\ldots\ldots (A\text{-}23)$$

$$C_j = [\bar{\theta}_{j-1}(z_{Dj-1},s) - Y_j(z_{Dj-1},s)]$$

$$\times\exp\{[s+\beta_j-D_j(s)]z_{Dj-1}\}, \; j=2,3\ldots n, \quad \ldots\ldots\ldots (A\text{-}24)$$

and $D_j(s) = \beta_j\omega_j K_0(\sqrt{\sigma_j s})/[\omega_j K_0(\sqrt{\sigma_j s}) + \sqrt{\sigma_j s}\,K_1(\sqrt{\sigma_j s})].$

$$\ldots\ldots\ldots\ldots\ldots\ldots\ldots\ldots\ldots (A\text{-}25)$$

Heat flux into (or from) the formation in Layer j is defined as

$$2\pi r_t q_j''(z,t) = -2\pi r_w K_j(\partial T_{2j}/\partial r)|_{r=r_w} \quad \ldots\ldots\ldots\ldots (A\text{-}26)$$

so that $q_j''(z,t) = [-K_j(T_{\text{inj}}-T_{\text{air}})/r_t](\partial\phi_j/\partial r_D)|_{r_D=1}$

$$= -U_j(T_{\text{inj}}-T_{\text{air}})[\phi_j(1,z_D,t_D) - \theta_j(z_D,t_D)]. \quad \ldots\ldots\ldots (A\text{-}27)$$

Total cumulative heat transfer is

$$Q_c(t) = \int_0^t \left[\sum_{j=1}^n \int_{z_{j-1}}^{z_j} 2\pi r_t q_j''(z,\tau)dz\right]d\tau. \quad \ldots\ldots\ldots\ldots (A\text{-}28)$$

For linear vertical-initial-temperature distributions in each layer of the formation, we can obtain the explicit form of the particular solution $Y_j(z,s)$ from Eq. 23. Then, the expressions for heat flux and total cumulative heat transfer in the Laplace-transformed space can be derived with Eqs. 24 and 25, respectively.

Appendix B—Analytical Solutions in Real Space

For a linear initial-temperature distribution in each layer of the formation, Eq. A-21 can be written as

$$\bar{\theta}_j(z_D,s) = \bar{A}_j(s) + [\bar{\theta}_{j-1}(z_{Dj-1},s) - \bar{A}_j(s)]\bar{B}_j(z_D,s),$$

$$j=1,2\ldots n \; (z_{Dj-1}\le z_D \le z_{Dj}), \quad \ldots\ldots\ldots\ldots (B\text{-}1)$$

where $\bar{A}_j(s) = -\{\delta_j/s[s+\beta_j-D_j(s)]\} = (1/s)\bar{f}_j(s)$

$$\times[\bar{f}_j(s) = s\bar{A}_j(s)], \quad \ldots\ldots\ldots\ldots\ldots\ldots\ldots (B\text{-}2)$$

$$\bar{B}_j(z_D,s) = \exp[-\beta_j(z_D-z_{Dj-1}]\exp[-s(z_D-z_{Dj-1})]$$

$$\times\exp[D_j(s)(z_D-z_{Dj-1})], \quad \ldots\ldots\ldots\ldots\ldots\ldots (B\text{-}3)$$

and $\bar{\theta}_0(z_{D0},s) = 1/s. \quad \ldots\ldots\ldots\ldots\ldots\ldots\ldots (B\text{-}4)$

The dimensionless temperature functions in the formation are

$$\bar{\phi}_j(r_D,z_D,t_D) = \bar{\theta}_j(z_D,s)\bar{g}_j(r_D,s), \; j=1,2\ldots n, \quad \ldots\ldots (B\text{-}5)$$

and $\bar{g}_j(r_D,s) =$

$$\omega_j K_0(\sqrt{\sigma_j s}\,r_D)/[\omega_j K_0(\sqrt{\sigma_j s}) + \sqrt{\sigma_j s}\,K_1(\sqrt{\sigma_j s})]. \quad \ldots\ldots (B\text{-}6)$$

Because the functions $\bar{A}_j(s)$, $\bar{B}_j(z_D,s)$, and $\bar{g}_j(r_D,s)$ have a branch point at the origin, we have to use the inversion theorem for Laplace transformations by evaluating the contour integral.[13] The following inversion can be proven after some algebraic operations.[14]

$$f_j(t_D) = \mathcal{L}^{-1}[\bar{f}_j(s)] = \frac{\delta_j}{2\pi i}\int_0^\infty e^{-t_D\lambda}[\bar{f}_j(\lambda e^{-i\pi}) - \bar{f}_j(\lambda e^{i\pi})]d\lambda$$

$$= \frac{4\delta_j}{\pi^2\sigma_j}\int_0^\infty e^{-(u^2/\sigma_j)t_D}\frac{uD_j^*(u)}{\left[D^*(u)\left(\beta_j-\dfrac{u^2}{\sigma_j}\right)R_j(u)\right]^2 + \dfrac{4}{\pi^2}}du.$$

$$\ldots\ldots\ldots\ldots\ldots\ldots\ldots\ldots\ldots (B\text{-}7)$$

$$\mathcal{L}^{-1}\{\exp[D_j(s)(z_D-z_{Dj-1})]\} = \frac{1}{2\pi i}\int_0^\infty e^{-t_D\lambda}$$

$$\times\{\exp[D_j(\lambda e^{-i\pi})(z_D-z_{Dj-1})] - \exp[D_j(\lambda e^{i\pi})(z_D-z_{Dj-1})]\}d\lambda$$

$$= \frac{2}{\lambda\sigma_j}\int_0^\infty u\sin\left[\frac{2(z_D-z_{Dj-1})}{\pi D_j^*(u)}\right]$$

$$\times\exp\left[(z_D-z_{Dj-1})R_j(u)/D_j^*(u) - \frac{u^2}{\sigma_j}t_D\right]du. \quad \ldots\ldots\ldots (B\text{-}8)$$

Then, $A_j(t_D) = \mathcal{L}^{-1}\left[\dfrac{1}{s}\bar{f}_j(s)\right] = \int_0^{t_D} f_j(\tau)d\tau = \dfrac{4\delta_j}{\pi^2}\int_0^\infty \dfrac{D^*(u)}{u}$

$$\times\frac{[e^{-(u^2/\sigma_j)t_D} - 1]}{\left[D_j^*(u)\left(\beta_j-\dfrac{u^2}{\sigma_j}\right) - R_j(u)\right]^2 + \dfrac{4}{\pi^2}} \quad \ldots\ldots\ldots\ldots (B\text{-}9)$$

and $B_j(z_D,t_D) = \mathcal{L}^{-1}[\bar{B}_j(z_D,s)] = \exp[-\beta_j(z_D-z_{Dj-1})]\mathcal{L}^{-1}$

$$\times\{\exp[-s(z_D-z_{Dj-1})]\exp[D_j(s)(z_D-z_{Dj-1})]\}$$

$$= \begin{cases} 0 \quad (t_D\le z_D-z_{Dj-1}) \\[2mm] \dfrac{2}{\pi\sigma_j}\exp[-\beta_j(z_D-z_{Dj-1})]\int_0^\infty u\sin\left[\dfrac{2(z_D-z_{Dj-1})}{\pi D_j^*(u)}\right] \end{cases}$$

$$\times\exp\left[(z_D-z_{Dj-1})R_j(u)/D_j^*(u) - \frac{u^2}{\sigma_j}(t_D-z_D+z_{Dj-1})\right]du,$$

$$t_D > z_D - z_{Dj-1}. \quad \ldots\ldots\ldots\ldots\ldots\ldots\ldots (B\text{-}10)$$

Taking the inverse Laplace transform of Eq. B-1 and using Eqs. B-9 and B-10 and the convolution property of the Laplace transform, we have

$$\theta_j(z_D,t_D) = \mathcal{L}^{-1}[\bar{\theta}_j(z_D,s)] = A_j(t_D) + \int_0^{t_D}[\theta_{j-1}(z_{Dj-1},\tau) - A_j(\tau)]$$

$$\times B_j(z_D,t_D-\tau)d\tau \quad \ldots\ldots\ldots\ldots\ldots\ldots\ldots (B\text{-}11)$$

Authors

Wu   **Pruess**

Yu-Shu Wu, postdoctoral fellow with the Earth Sciences Div. of the Lawrence Berkeley Laboratory, has research interests in mathematical modeling and transport phenomena of multiphase and multicomponent fluids in porous media. He holds BS and MS degrees in petroleum engineering from the Petroleum Inst. in China, and MS and PhD degrees in hydrogeology from the U. of California, Berkeley. **Karsten Pruess** is a staff scientist in the Earth Sciences Div. of Lawrence Berkeley Laboratory. His research interests include modeling subsurface flow systems. He previously was a researcher and lecturer at the U. of Bremen and the U. of Frankfurt in West Germany. He holds a PhD degree in physics from the U. of Frankfurt. Pruess was a member of the 1985–89 Editorial Review Committee and is on the program committee for the 1991 Symposium on Reservoir Simulation.

and $g_j(r_D,t_D) = \mathcal{L}^{-1}[\bar{g}_j(r_D,s)] = \dfrac{1}{2\pi i}\int_0^\infty e^{-t_D\lambda}[\bar{g}_j(r_D,\lambda e^{-i\pi})$

$$-\bar{g}_j(r_D,\lambda e^{i\pi})]d\lambda = \frac{2}{\pi\sigma_j\beta_j}\int_0^\infty \frac{ue^{-(u^2/\sigma_j)t_D}}{D^*(u)}$$

$$\times\{Y_0(ur_D)[\omega_j J_0(u)+uJ_1(u)]-J_0(ur_D)[uY_1(u)+\omega_j Y_0(u)]\}du$$

$$\dots\dots\dots\dots\dots\dots\dots\dots\dots\dots\dots\text{(B-12)}$$

Then, $\phi_j(r_D,z_D,t_D) = \displaystyle\int_0^{t_D}\theta_j(z_D,\tau)g_j(r_D,t_D-\tau)d\tau.\quad\dots\text{(B-13)}$

In the above solutions,

$$R_j(u) = J_0(u)[\omega_j J_0(u)+uJ_1(u)]+Y_0(u)[\omega_j Y_0(u)+uY_1(u)]$$

$$\dots\dots\dots\dots\dots\dots\dots\dots\dots\dots\dots\text{(B-14)}$$

and $D_j^*(u) = \{[\omega_j Y_0(u)+uY_1(u)]^2$

$$+[\omega_j J_0(u)+uJ_1(u)]^2\}/\beta_j\omega_j.\quad\dots\dots\dots\dots\dots\dots\text{(B-15)}$$

For Layer 1, the solution in Eq. B-11 is simplified to Eq. 26.

SPERE